0026-895X/07/7206-1522–1534$20.00
MOLECULAR PHARMACOLOGY
Copyright © 2007 The American Society for Pharmacology and Experimental Therapeutics
Mol Pharmacol 72:1522–1534, 2007

Vol. 72, No. 6
39388/3278528
Printed in U.S.A.

The Molecular Basis of High-Affinity Binding of the Antiarrhythmic Compound Vernakalant (RSD1235) to Kv1.5 Channels

Jodene Eldstrom, Zhuren Wang, Hongjian Xu, Marc Pourrier, Alan Ezrin, Ken Gibson, and David Fedida

Department of Anesthesiology, Pharmacology and Therapeutics, University of British Columbia, Vancouver, British Columbia, Canada (J.E., Z.W., H.X., D.F.); and Cardiome Pharma Corp., Vancouver, British Columbia, Canada (M.P., A.E., K.G.)

Received July 3, 2007; accepted September 14, 2007

ABSTRACT

Vernakalant (RSD1235) is an investigational drug recently shown to convert atrial fibrillation rapidly and safely in patients (*J Am Coll Cardiol* **44:**2355–2361, 2004). Here, the molecular mechanisms of interaction of vernakalant with the inner pore of the Kv1.5 channel are compared with those of the class IC agent flecainide. Initial experiments showed that vernakalant blocks activated channels and vacates the inner vestibule as the channel closes, and thus mutations were made, targeting residues at the base of the selectivity filter and in S6, by drawing on studies of other Kv1.5-selective blocking agents. Block by vernakalant or flecainide of Kv1.5 wild type and mutants was assessed by whole-cell patch-clamp experiments in transiently transfected human embryonic kidney 293 cells. The mutational scan identified several highly conserved amino acids, Thr479, Thr480, Ile502, Val505, and Val508, as important residues for affecting block by both compounds. In general, mutations in S6 increased the IC_{50} for block by vernakalant; I502A caused an extremely local 25-fold decrease in potency. Specific changes in the voltage-dependence of block with I502A supported the crucial role of this position. A homology model of the pore region of Kv1.5 predicted that, of these residues, only Thr479, Thr480, Val505, and Val508 are potentially accessible for direct interaction, and that mutation at additional sites studied may therefore affect block through allosteric mechanisms. For some of the mutations, the direction of changes in IC_{50} were opposite for vernakalant and flecainide, highlighting differences in the forces that drive drug-channel interactions.

Atrial fibrillation, the most common sustained cardiac arrhythmia, is associated with ~15% of all strokes (Kannel et al., 1998; Go et al., 2001; Rockson and Albers, 2004) and occurs in approximately 30% of patients after cardiac surgery (Leung et al., 2004). Most drugs currently in use for treatment of atrial fibrillation are indiscriminate, targeting channels in both atrial and ventricular tissue and are therefore associated with life-threatening (ventricular) arrhythmias. Vernakalant (RSD1235) is a mixed voltage- and frequency-dependent Na^+ and atria-preferred K^+ channel blocker (Roy et al., 2004; Fedida et al., 2005) under development for the acute conversion of atrial fibrillation to sinus rhythm. In recent phase II and III clinical trials, vernakalant has shown promise as an intravenous antiarrhythmic agent for rapid conversion of atrial fibrillation to sinus rhythm with an overall rate close to 52% within 90 min of infusion, compared with a placebo conversion rate of just 3.8% (Roy et al., 2005; Pratt et al., 2006; Stiell et al., 2006; Fedida, 2007). Previous studies have shown that one of the actions of vernakalant is block of the atria-specific I_{Kur} current (Fedida et al., 2005), which in human atria is thought to be the result of expression of the *KCNA5* gene and Kv1.5 protein (Fedida et al., 1993; Feng et al., 1997). Evidence suggests that the safety of this drug is in part related to the higher sensitivity of atria-specific Kv1.5 to block by vernakalant over other channels involved in ventricular repolarization, such as hERG (Fedida et al., 2005) and KCNQ1.

This work was supported by a research grant from Cardiome Pharma Corp, and operating grants from the Heart and Stroke Foundations of British Columbia and Yukon and the CIHR. D.F. was supported by a Career Investigator Award from the Heart and Stroke Foundation of Canada.

J.E. and Z.W. contributed equally to the execution and interpretation of this study.

Article, publication date, and citation information can be found at http://molpharm.aspetjournals.org.

doi:10.1124/mol.107.039388.

ABBREVIATIONS: RSD1235, vernakalant [(3*R*)-1-[(1*R*,2*R*)-2-[2-(3,4-dimethoxyphenyl)ethoxy]cyclohexyl]pyrrolidin-3-ol hydrochloride]; HEK, human embryonic kidney; MEM, minimal essential medium; WT, wild type; S0100176, *N*-benzyl-*N*-pyridin-3-ylmethyl-2-(toluene-4-sulfonylamino)-benzamide hydrochloride; AVE0118, (2'-{[2-(4-methoxy-phenyl)-acetylamino]-methyl}-biphenyl-2-carboxylic acid (2-pyridin-3-yl-ethyl)-amide; AZD7009, *tert*-butyl-2-(7-[(2*S*)-3-(4-cyanophenoxy)-2-hydroxypropyl]-9-oxa-3,7-diazabicyclo[3.3.1]non-3-yl)ethylcarbamate.

Several antiarrhythmic drugs in development [S0100176 (Decher et al., 2004), AVE0118 (Decher et al., 2006), and AZD7009 (Persson et al., 2005)], some well known agents [quinidine (Snyders et al., 1992; Fedida, 1997) and flecainide (Grissmer et al., 1994)], and the local anesthetics bupivacaine (Franqueza et al., 1997) and benzocaine (Caballero et al., 2002), have been shown to block Kv1.5 also. The potency of these agents is affected by introduction of specific mutations in the S6 domain of Kv1.5, which lines the inner vestibule of the channel (Val505, Thr507, Ile508, Leu510, Val512, Val514), or mutations in the deep pore (Thr479 and Thr480) near the selectivity filter (Yeola et al., 1996; Franqueza et al., 1997; Caballero et al., 2002; Decher et al., 2004, 2006; Herrera et al., 2005). Many of these same residues are also important sites of interaction for the Kvβ inactivation particle (Decher et al., 2005), for tetraethylammonium (Choi et al., 1993; Lopez et al., 1994), and for 4-aminopyridine block (Kirsch and Drewe, 1993).

Flecainide is also a drug of choice for the acute conversion of atrial fibrillation to sinus rhythm (Fuster et al., 2006) and is known to block Kv1.5 (Grissmer et al., 1994; Herrera et al., 2005) but with much lower potency than vernakalant. In the present study, we have investigated the binding site of vernakalant in the deep pore and S6 of Kv1.5 using both electrophysiology and site-directed mutagenesis. Flecainide has been used as a comparator compound to validate our data against that already present in the literature, and also to extend studies of flecainide block itself. The results demonstrate that Ile502 in the S6 domain is a key residue in the block of Kv1.5 by vernakalant, but less so for flecainide. We have interpreted our results in the context of the hydrophobicity, size, and potential for cation-π interactions of the different substituted residues, and we have extended our analysis by carrying out homology modeling and ligand docking of vernakalant on Kv1.5 based on the published crystal structure of Kv1.2 (Long et al., 2005).

Materials and Methods

Cell Preparation. Stable lines of HEK 293 cells expressing Kv1.5 or transient transfection of mutant Kv1.5 channels was used in all experiments. Primers to generate mutant channels were synthesized by Integrated DNA Technologies, Inc. (Coralville, IA), and mutants were generated using the QuikChange kit (Stratagene, La Jolla, CA). The presence of the mutation was confirmed by DNA sequencing, and because of the size of the WT Kv1.5 clone, only the sequenced region harboring the targeted nucleotides was subcloned as a fragment back into full-length Kv1.5. Transient transfections were performed with HEK 293 cells plated at 20 to 30% confluence on sterile coverslips in 25 mm Petri dishes 1 day before transfection. Ion channel DNA (0.1 to 4 μg) was incubated with 1 μg of enhanced green fluorescent protein DNA (to enable detection of transfected cells) and 2 μl of Lipofectamine 2000 (Invitrogen, Mississauga, ON, Canada) in 100 μl of OptiMEM. This was added to the cells for overnight incubation after washing the cells with 900 μl of minimal essential medium (MEM) with 10% FBS.

The cells were grown in MEM at 37°C in an air/5% CO_2 incubator. Media contained 10% bovine serum and 0.5 mg/ml Geneticin (G-418) for stable lines. On the day before recording, stably expressing cells were washed with MEM, treated with trypsin/EGTA for 1 min, and plated on 25-mm^2 coverslips. All cell culture supplies were obtained from Invitrogen.

Drugs and Solutions. Control bath solution contained 5 mM KCl, 135 mM NaCl, 2.8 mM sodium acetate, 1 mM $MgCl_2$, 10 mM HEPES, and 1 mM $CaCl_2$, adjusted to pH 7.4 with NaOH. Patch pipettes contained 130 mM KCl, 5 mM EGTA, 1 mM $MgCl_2$, 10 mM HEPES, 4 mM Na_2ATP, and 0.1 mM GTP, adjusted to pH 7.2 with KOH. All chemicals used to make solutions were obtained from Sigma-Aldrich (Mississauga, ON, Canada). Vernakalant (RSD1235; lot numbers DM-155-A and JL-78-12) was synthesized by Cardiome Pharma Corp. (Vancouver, BC, Canada) and prepared as a stock solution (50 mM) in H_2O. Flecainide (Sigma-Aldrich; lot number 094K4057) was prepared as a stock solution (100 mM) in 100% dimethyl sulfoxide, concentrations of which never exceeded 0.1% (v/v) in the final experimental solutions.

Whole-Cell Patch-Clamp Recordings. Coverslips with adherent cells plated on the surface were placed in a superfusion chamber (volume, 300 μl) containing the control bath solution at 22°C. Whole-cell current recording and analysis were carried out using an Axopatch 200B amplifier and pClamp10 software (Molecular Devices, Sunnyvale, CA). Patch electrodes were pulled from thin-walled borosilicate glass (World Precision Instruments, Sarasota, FL) on a horizontal micropipette puller (Sutter Instrument Company, Novato, CA). Electrodes had resistances of 1.0 to 3.0 MΩ when filled with control filling solution. Analog capacity compensation and 80% series resistance compensation were used during whole-cell measurements. Membrane potentials were not corrected for junction poten-

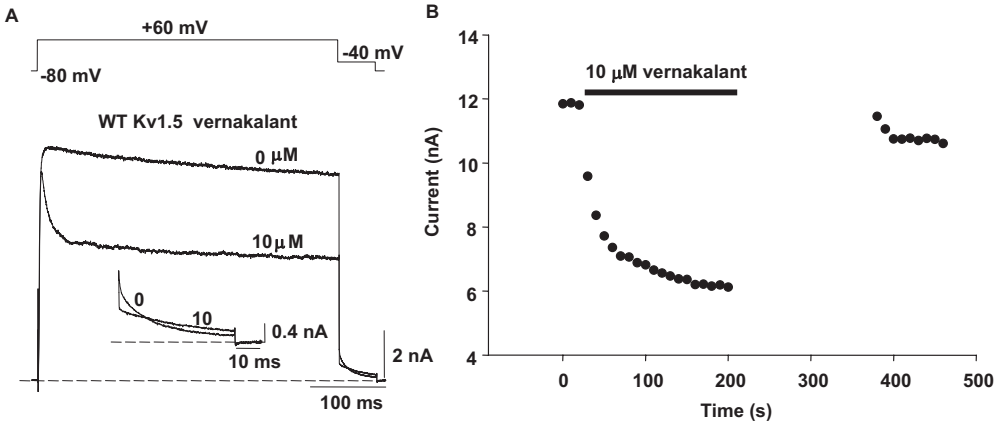

Fig. 1. Tail current cross-over reveals an inner pore site of access for vernakalant. A, voltage protocol for recording of Kv1.5 currents from HEK cells. Cells were held at −80 mV and pulsed to +60 mV for 400 ms before repolarizing to −40 mV to record tail currents. Protocol was repeated at 0.1-Hz intervals. Current traces in the bottom panel were obtained in control and after 5-min exposure to 10 μM vernakalant. Inset shows tail currents at −40 mV in control and vernakalant on an expanded time base to highlight crossover. In this figure as in all others, numbers adjacent to tracings refer to drug concentrations in micromolar unless otherwise stated. B, diary plot of steady-state Kv1.5 current at the end of 400-ms depolarizations. Pulse frequency was 0.1 Hz. Between 200 and 380 s, the cell was rested at −80 mV while vernakalant was washed out of the bath.

tials that arise between the pipette and bath solution. For Kv1.5 current recordings, a holding potential of −80 mV was used. Data were sampled at 10 to 20 kHz and filtered at 5 to 10 kHz. To assess drug block, half-log escalating concentrations of drug were added to the flowing bath solution, and current traces were recorded with 400 ms depolarizing pulses to +60 mV at a frequency of 0.1 Hz. Concentrations approximately equal to the 50% inhibitory value for each drug on the WT channel were used in the initial investigation of vernakalant and flecainide actions on mutated channels.

Data Analysis. Data are represented as mean ± S.E.M. unless otherwise specified. For significance of differences, * represents $p < 0.05$ and ** represents $p < 0.01$; statistical analysis was conducted using Student's t test (unpaired). Clampfit software (Molecular Devices) was used to analyze current traces. Data from each test pulse (currents in the presence of drug) were normalized to control test pulse currents obtained before drug exposure. For drug potency studies of the mutant Kv1.5 channels in the presence of vernakalant or flecainide (Figs. 3 and 4), currents in the presence of different concentrations of drug were normalized to the current in control and used to generate concentration-response curves for changes in steady state Kv1.5 current. The resulting concentration-response relations were computer-fitted to the Hill equation: $i = 1/[1 + (IC_{50}/[D]^{n_H})]$, where i is the normalized current recorded ($i = I_{drug}/I_{control}$) at drug concentration [D], IC_{50} is the concentration producing half-maximal inhibition, and n_H is the Hill coefficient.

The voltage dependence of block for vernakalant and flecainide was determined by the calculation of the fractional block ($f = 1 - I_{drug}/I_{control}$) at the potentials in the range of full channel opening (between +10 and +60 mV) and fitting the data to the Woodhull equation: $f = [D]/([D] + K_d{*}e^{-\delta zFE/RT})$, where δ is the fractional electrical distance (i.e., the fraction of the transmembrane electrical field sensed by a single charge at the receptor site), z is the effective valence of the cytoplasmic blocker, F is the Faraday constant, E is the imposed voltage, R is the universal gas constant, T is absolute temperature, and $K_d{*}$ represents the binding affinity at the reference voltage (0 mV). The current amplitude (I_{drug} and $I_{control}$) was measured at the end of a 400-ms depolarization.

Homology Model. The Kv1.5 homology model was generated using "First Approach Mode" of SWISS-MODEL (http://swissmodel.expasy.org) and the three-dimensional structure of rKv1.2 (Protein Data Bank code 2A79; Long et al., 2005), which is believed to represent the open state of the channel. rKv1.2 and hKv1.5 show 100% identity in S5 and S6 and 88% identity in the pore loop. The figure was generated using DeepView Swiss-PdbViewer (http://swissmodel.expasy.org/spdbv) and Adobe Photoshop software (Adobe Systems, Mountain View, CA). This homology model was used for docking of vernakalant using Chem Bio3D (CambridgeSoft Corporation, Cambridge, MA), AutoDock tools, and AutoDock4 (http://autodock.scripps.edu; Morris et al., 1998). A lowest-energy conformation of vernakalant, protonated on the nitrogen atom as it would be at physiological pH, was used for docking. The channel macromolecule remained rigid during the docking computation, whereas vernakalant was flexible.

Results

Delayed Closing of Kv1.5 Channels in the Presence of Vernakalant at the Inner Pore. It was suggested from our previous experiments that block of Kv1.5 by vernakalant was mediated after channel activation, because vernakalant caused a relatively rapid onset of block of channel current upon depolarization (Fedida et al., 2005) but little evidence of resting or "tonic" block of the channel. The activation gate of Kv channels is known to lie on the intracellular side of the pore (Holmgren et al., 1998), and thus a requirement for channel activation for block to occur suggests intracellular access of the drug to the pore region of the channel. In our initial experiments aimed at localizing the site of binding of vernakalant within Kv1.5, we

TABLE 1
Summary of fractional block and IC_{50} values for block by vernakalant of wild-type and mutant Kv1.5 channels
Fractional block was measured at 10 μM vernakalant. Values are expressed as mean ± S.E.M.

	Fractional Block	Significance	n	IC_{50}	Hill Coefficient	-Fold change	n
				μM			
WT	0.45 ± 0.03		23	13.35 ± 0.93	1.00		5–23
T479A	0.77 ± 0.05	$P < 0.01$	9	1.63 ± 0.09	0.6	8.31	5–10
T479S	0.23 ± 0.04	$P < 0.01$	7	41.02 ± 3.54	0.95	3.07	3–8
T480A	0.23 ± 0.04	$P < 0.01$	12	52.59 ± 7.85	0.88	3.94	3–12
T480S	0.25 ± 0.07	$P < 0.05$	6	52.83 ± 12.46	0.64	3.96	4–7
V481L	0.36 ± 0.03		6				
C500A	0.21 ± 0.04	$P < 0.01$	10	45.63 ± 4.06	0.95	3.42	3–10
A501V	0.69 ± 0.04	$P < 0.01$	8	3.49 ± 0.19	0.85	3.81	4–8
I502A	0.07 ± 0.03	$P < 0.01$	9	329.26 ± 18.97	0.65	24.66	4–10
I502L	0.33 ± 0.07		6	24.84 ± 3.14	0.96	1.86	3–6
I502F	0.10 ± 0.01	$P < 0.01$	4	149.29 ± 8.36	0.84	11.11	4
I502K	D.N.E.		6				
I502D	D.N.E.		5				
V505A	0.21 ± 0.04	$P < 0.01$	10	45.54 ± 2.56	0.95	3.41	3–10
V505L	0.22 ± 0.07	$P < 0.05$	4	57.70 ± 4.63	0.77	4.32	3–5
V505F	0.27 ± 0.05	$P < 0.05$	6	28.79 ± 0.79	0.96	2.16	5–6
V505K	D.N.E.		5				
V505D	D.N.E.		5				
I508A	0.21 ± 0.03	$P < 0.01$	8	42.44 ± 0.94	0.87	3.18	3–8
I508L	0.38 ± 0.05		4	16.84 ± 0.48	1.00	1.26	3–4
I508Y	0.21 ± 0.03	$P < 0.01$	7	24.70 ± 0.63	1.46	1.85	4–7
I508F	0.94 ± 0.02	$P < 0.01$	5	0.61 ± 0.03	1.23	21.80	4–8
I508K	D.N.E.		5				
I508D	D.N.E.		5				
A509G	0.33 ± 0.07		9				
A509V	D.N.E.		12				
V512L	0.56 ± 0.04		9				
P532L	0.26 ± 0.03	$P < 0.01$	16	32.02 ± 1.83	0.96	2.40	3–16

D.N.E., did not express.

have examined the ability of the drug to affect activation gate closure upon repolarization, after channel opening (Fig. 1). Control currents in Fig. 1A activate rapidly upon depolarization to +60 mV and show only limited inactivation during the 400-ms depolarization shown here. During repolarization to −40 mV, a deactivation tail current is observed that reflects channel clo-

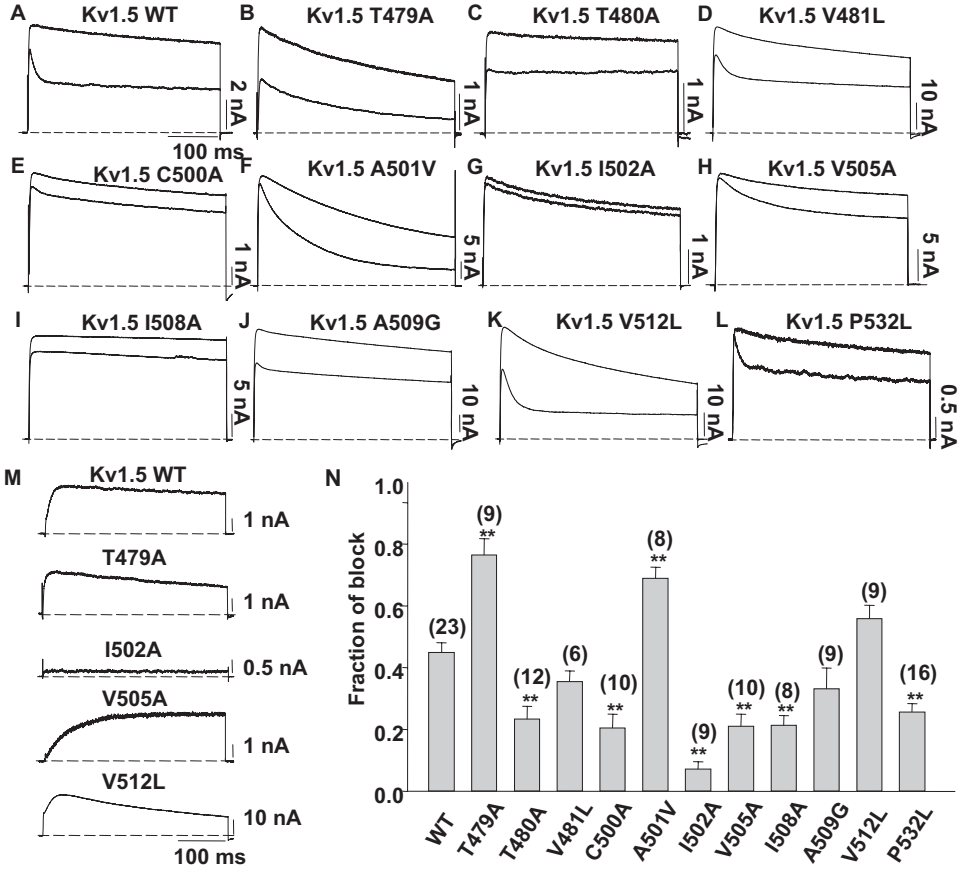

Fig. 2. Alanine scan of pore-S6 with 10 μM vernakalant. A–L, Kv1.5 currents in control and in the presence of 10 μM vernakalant in each case. Cells were pulsed from −80 to +60 mV for 400 ms at 0.1 Hz. Channel mutation is identified above each pair of current tracings. See Table 1 for complete results, including a listing of nonexpressing mutants. M, difference currents showing the vernakalant-sensitive currents for a selection of the mutants in A, as labeled. N, bar graph of fraction of Kv1.5 current block by 10 μM vernakalant. Numbers in brackets denote number of cells studied and are shown ± S.E.M. **, $p < 0.01$ compared with control block.

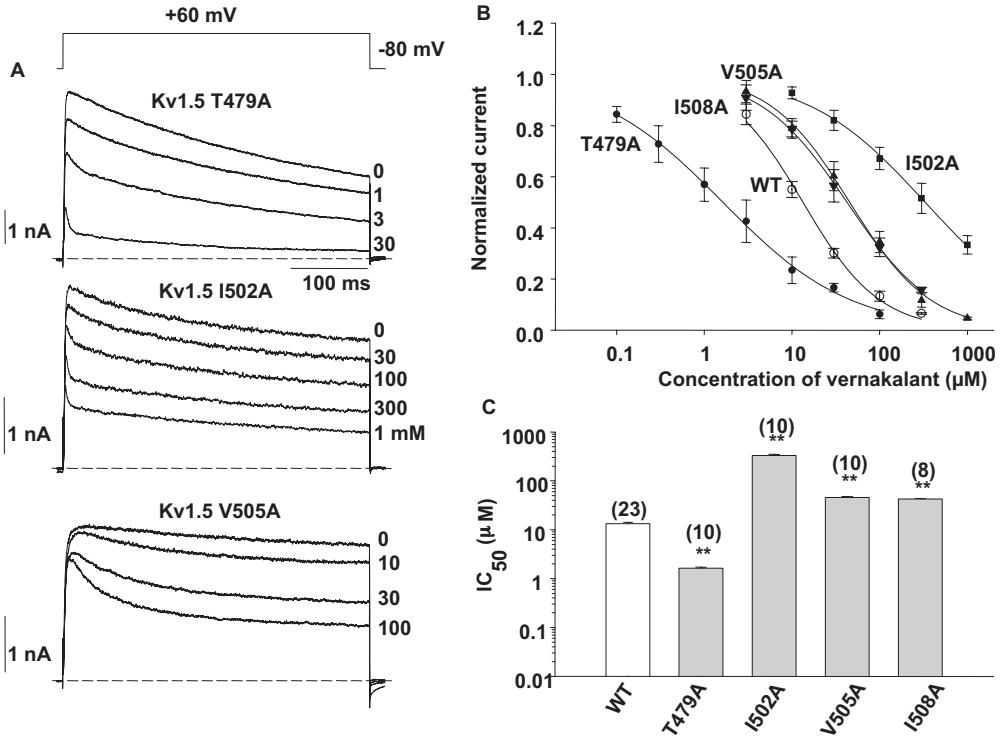

Fig. 3. Dose-response relationships for vernakalant on selected Kv1.5 mutant channels. A, selected current tracings from T479A, I502A, and V505A mutant Kv1.5 channels exposed to increasing concentrations of vernakalant. Cells were held at −80 mV and pulsed to +60 mV as indicated in the protocol at top. In this figure as in all others, numbers adjacent to tracings refer to drug concentrations in micromolar unless otherwise stated. B, dose response relationships obtained from data tracings as in A were normalized and plotted versus log [vernakalant], and fitted to a Hill equation (see *Materials and Methods* for details). Data points are shown ± S.E.M. IC_{50} values may be found in the text and Table 1. C, bar graph comparing IC_{50} values for mutant Kv1.5 channels exposed to vernakalant. Numbers in parentheses refer to the number of cells studied and are shown ± S.E.M. **, $p < 0.01$ compared with control IC_{50} value.

sure. In the presence of 10 μM vernakalant, rapid block is apparent after channel opening, and a steady-state current level is rapidly reached. Upon repolarization, the tail current amplitude is initially less than in control, but decays more slowly and crosses over the control tracing as it declines to the baseline current level (Fig. 1, inset). The result suggests that vernakalant delays closing of Kv1.5 and, perhaps, that the channels cannot close while vernakalant is bound; they may require drug expulsion from the inner vestibule before that can happen.

This possibility was tested in the experiment shown in Fig. 1B. Here, after equilibration at 0.1 Hz in control solutions, the cell was exposed to vernakalant as shown. This led to a progressive reduction of steady-state current, and at 200 s, the cell was rested for 3 min at −80 mV and vernakalant was washed from the bath. When the current was activated again by depolarizing clamp pulses, the current level was immediately restored to the control level. This suggests that vernakalant was not trapped in the closed channels while drug was washed from the bath, but rather that, as channels closed, vernakalant was slowly expelled from the inner pore. This slow expulsion is the cause of the slowed tail current observed in the presence of vernakalant (Fig. 1A).

Alanine Scan of S6: Block by Vernakalant. The data in Fig. 1 suggest that the S6 domain that lines the inner vestibule of the channel and the deep pore near the selectivity filter are likely areas where vernakalant could bind to Kv1.5. Extensive studies of some approved and developmental antiarrhythmic agents that target either the cardiac Na^+ channel or K^+ channels involved in action potential repolarization have suggested that the base of the selectivity filter in the deep pore and the S6 are important areas for antiarrhythmic drug binding within the ion conduction pathway (Decher et al., 2004; Herrera et al., 2005). These regions were targeted for mutational analysis of block by replacement of WT residues with alanines wherever possible, valines if the WT residue was an alanine, and leucine, valine, or glycine if there was an expression problem with alanine. A summary of the mutants used in the present experiments is shown in Table 1 and includes those that we were unable to record current from. Channels transiently or stably (see *Materials and Methods*) expressed in HEK cells were voltage-clamped with depolarizing pulses from −80 to +60 mV at 0.1 Hz and allowed to equilibrate for 5 min before drugs were applied. Control currents in Fig. 2 show some differences among mutants. Most of the examples show the rapidly activating, delayed-rectifier current expected from Kv1.5 channels, with a minor degree of slow inactivation occurring during the 400-ms depolarizations used here. However, a few channels, Kv1.5 T479A, A501V, and V512L, showed a definite increase in inactivation rate.

At first, a scan of residues using 10 μM vernakalant was carried out to generally assess the importance of residues in this area. This concentration reduced currents significantly in almost all mutants studied, with an approximately 50% reduction of outward current in WT channels, as has been previously reported (Fedida et al., 2005), and reduced block in most other mutants with the least effect on the I502A mutant (Fig. 2G). Difference currents for some example mutants are shown in Fig. 2M, showing the different levels of block; here, the increased inactivation rate induced by the V512L mutation is apparent as a decaying difference current during the pulse. It was noted that the three mutants with increased inactivation all showed greater block at 10 μM vernakalant than control, and this finding is clearly seen in the bar graph, which summarizes data from the S6 mutations (Fig. 2N). As well, Thr479 and Thr480 are located at the

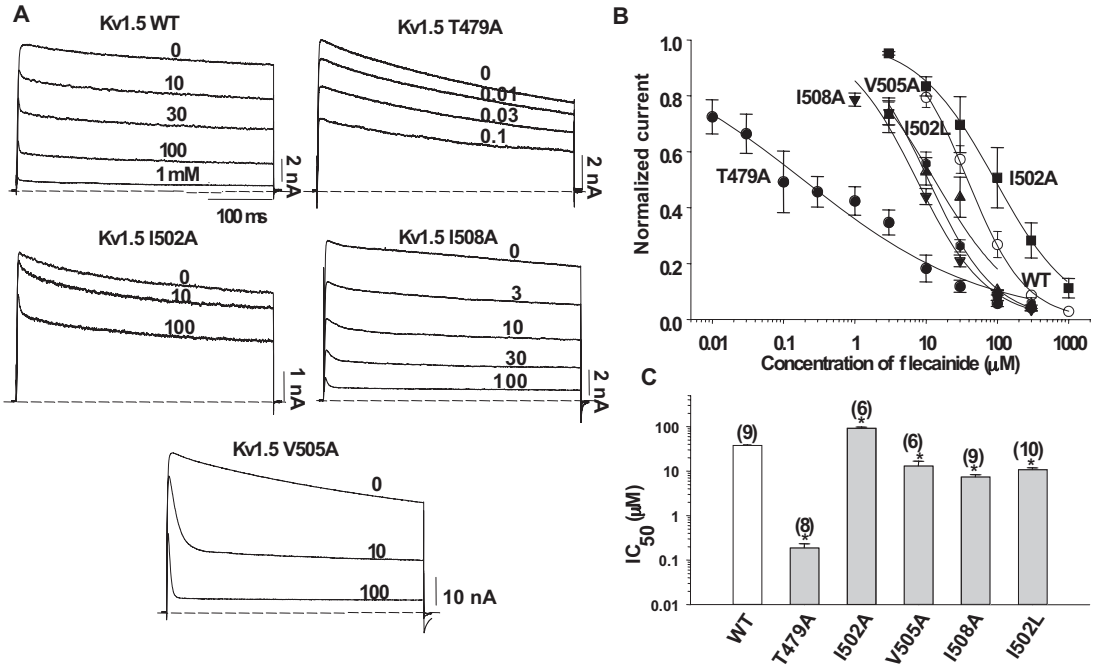

Fig. 4. Dose-response relationships for flecainide on selected Kv1.5 mutant channels. A, selected current tracings from Kv1.5 WT, T479A, I502A, V505A, and I508A mutant Kv1.5 channels exposed to increasing concentrations of flecainide. Cells were held at −80 mV and pulsed to +60 mV. B, dose response relationships obtained from data tracings as in A were normalized and plotted versus log [flecainide], and fitted to a Hill equation (see *Materials and Methods* for details). Data points are shown ± S.E.M. IC_{50} values may be found in the text and Table 2. C, bar graph comparing IC_{50} values for mutant Kv1.5 channels exposed to flecainide. Numbers in parentheses refer to the number of cells studied, and are shown ± S.E.M. *, $p <$ 0.05 compared with control IC_{50} value.

inner mouth of the selectivity filter, and any changes that these mutations induce in K^+ selectivity or permeation might have independent actions on drug block. As a result, the data from these mutants, although of interest in this study, are subject to the caveat above when being compared with the potency data from other mutations in the remaining experiments.

Significant reductions in block by 10 μM vernakalant appeared to be centered on Ile502, with a diminishing effect for mutations moving away from this site, disappearing distally along S6 by residue Ala509 and proximally by residues Val481 and Cys500 at the base of the selectivity filter.

TABLE 2
Summary of IC_{50} values for block by flecainide for wild-type and mutant Kv1.5 channels

	IC_{50}	Significance	-Fold Change	n
	μM			
WT	38.14 ± 1.06			6–9
T479A	0.19 ± 0.04	$P < 0.001$	200	3–8
I502A	92.04 ± 5.54	$P < 0.001$	2.43	3–6
I502L	10.75 ± 1.09	$P < 0.001$	3.55	5–10
I502F	164.49 ± 31.36	$P < 0.001$	4.13	3–6
V505A	13.076 ± 3.58	$P < 0.001$	2.92	4–6
V505F	4.27 ± 0.34	$P < 0.001$	8.93	4–6
I508A	7.39 ± 0.92	$P < 0.001$	5.15	3–9
I508F	74.71 ± 5.37	$P < 0.001$	1.96	4–9

Full dose-response relationships for vernakalant (Fig. 3) were obtained for the reduced block mutants, I502A, V505A, and I508A, in comparison with a positive control mutation that increased block (T479A), and for a readily available comparative antiarrhythmic agent, flecainide (Fig. 4), whose block is also reported to be affected by mutations in the lower S6 (Herrera et al., 2005). Vernakalant data in Fig. 3 confirmed the 10 μM scan in Fig. 2, with increased potency for T479A and with reduced potency for the other mutants. Original tracings are shown in Fig. 3A and illustrate the actions of vernakalant at concentrations between 1 μM and 1 mM in the different mutants. Steady-state current block was plotted against drug concentration (Fig. 3B) and fitted with a Hill equation to obtain the IC_{50} values for the different mutants, which are also shown in the bar graph below (Fig. 3C).

The most important effect was the reduction in potency for vernakalant centered at I502A, which had an IC_{50} of 329 ± 19 μM (n = 4–10, see Table 1), compared with a control IC_{50} of 13.4 ± 0.9 μM (n = 5–23), which is a 25-fold decrease in potency. V505A, I508A, T480A, and C500A showed lesser reductions in potency on Kv1.5 (Table 1), of between 3- and 4-fold (Table 1). Similar experiments were carried out for flecainide (Fig. 4A), and in qualitative agreement with previous oocyte data from Val481, the nearby residue in the selectivity filter (Herrera et al., 2005), the mutation of Thr479 to alanine increased the potency of flecainide (Fig. 4,

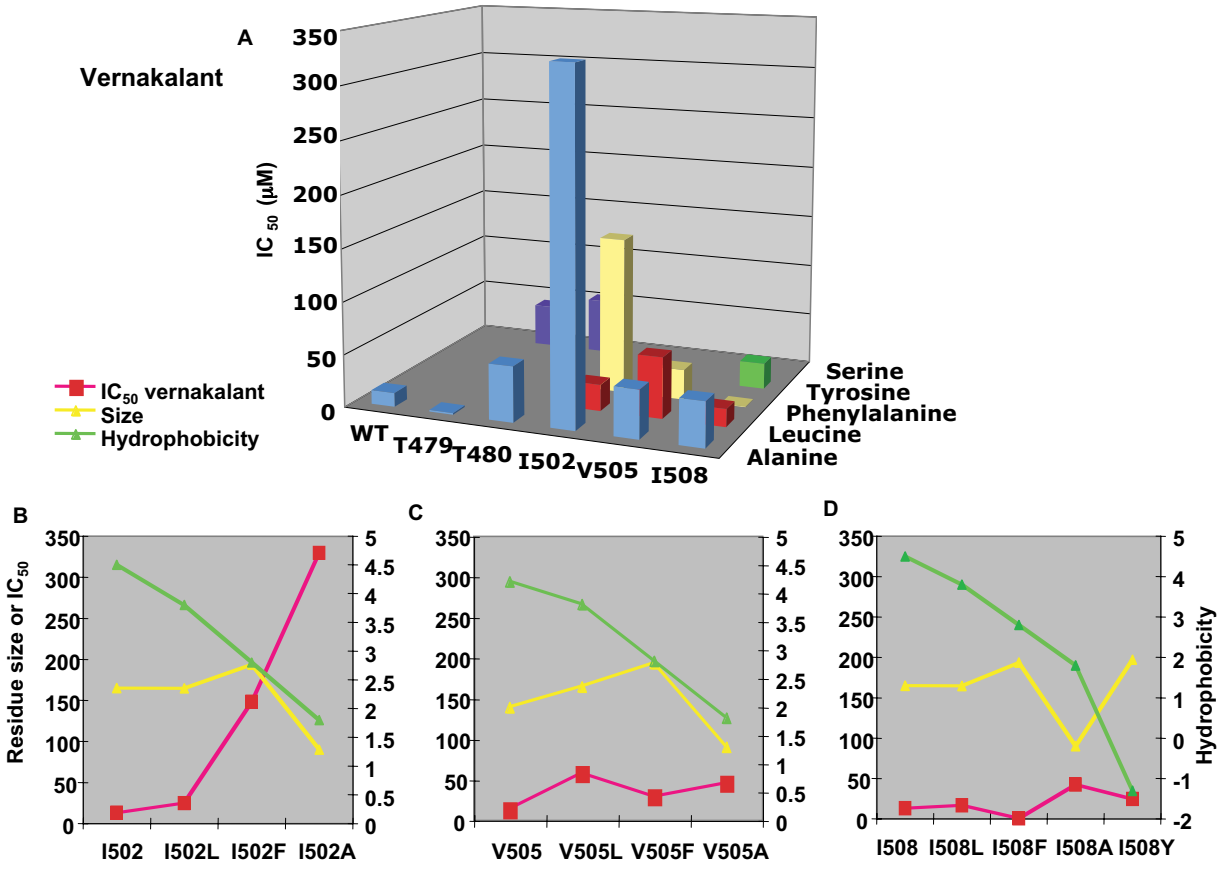

Fig. 5. Various amino acid substitutions to selected residues in S6, and their block by vernakalant. A, three-axis graph of the effect of different amino acid substitutions of the WT residues (abscissa) on the resultant mutant Kv1.5 channel IC_{50} (ordinate) for block by vernakalant. Note color coding of substituted residues, with WT and alanine mutants in pale blue: red, leucine; yellow, phenylalanine; green, tyrosine; dark blue, serine. B, correlation graphs comparing vernakalant IC_{50} (left ordinate, micromolar) versus hydrophobicity (right ordinate, Kyte-Doolittle units) and size (left ordinate, cubic Ångstroms) for a range of amino acids substituted at Ile502 (B), Val505 (C), and Ile508 (D). Spearman correlation coefficients: for Ile502 for size and hydrophobicity were −0.4 and −1.0, respectively; for Val505, r = 0.0 and −0.4; for Ile508, r = −0.4, and −0.6 (−1.0 without Tyr).

B and C), in this case by 238-fold, from a control IC_{50} of 38.1 ± 1.1 μM (n = 6–9, see Table 2) to 0.19 ± 0.04 μM (n = 3–8). I502A showed a diminished potency in the presence of flecainide, with an increase in IC_{50} from 38.1 μM in control to 92 ± 5.5 μM (n = 3–6), a 2.4-fold reduction in potency (Fig. 4, B and C). The effect of this mutation on flecainide block was clearly much less than on vernakalant block, and in a related area, insertion of alanines at Val505 and Ile508 increased the potency for flecainide block by 3- and 5.2-fold, respectively (Fig. 4C), in contrast to the reduction in block of 3- to 4-fold observed for vernakalant (Fig. 3C).

Further Examination of Other Amino Acid Substitutions in S6 on the Potency of Vernakalant and Flecainide Action. Given the obvious importance of Ile502 in the block by vernakalant, a series of other residues were substituted for isoleucine at this site, and close by, to alter the hydrophobicity, the residue size, and the potential for cation-π interactions in this region. The results for vernakalant are shown in Fig. 5, and comparative data for flecainide in Fig. 6 (see also Table 1). For substitutions at Ile502, there is a clear modulation of the vernakalant IC_{50} that is inversely related to the hydrophobicity of the substitution made, the native isoleucine (most hydrophobic) conferring the most potent block and alanine (most hydrophilic), the least potent block. Overall, the potency series is Ile > Leu > Phe > Ala (Fig. 5B). At Val505, a similar trend can be seen, albeit less marked, and at Ile508, no such correlation is apparent (Fig. 5, B and C). In contrast, cation-π interactions appear unimportant at Ile502 but become increasingly important moving to 505 and 508 (Fig. 5, A, C, and D), such that the potency for vernakalant on I508F was 0.61 μM, the highest obtained in the present series of experiments (Fig. 5A and Table 1). This result suggests that π-stacking between aromatic groups of the drug and I508F confers high-affinity binding. As well, at Ile508, a good correlation is apparent between vernakalant IC_{50} and residue size, which suggests that decreasing side-chain volume at this location causes some steric hindrance (Fig. 5D).

In the case of flecainide, there is no obvious correlation with the hydrophobicity of the substitution at Ile502, Val505, or Ile508 (Fig. 5, A–D). However, in contrast to vernakalant, residue size seems to correlate linearly with flecainide IC_{50} values at position 508 (Fig. 6D), and inversely with IC_{50} at position 505. There is also the suggestion that size is important for flecainide IC_{50} at position 502, where directional changes in potency match the size change from residue to residue (Fig. 6B). Cation-π interactions seem less important for flecainide than for vernakalant, or the geometric needs are more specific; i.e., the aromatic needs to be a specific distance from other sites of interaction. V505F seems to be an exception to this, where the IC_{50} value is 4.3 μM, compared with 38 μM in the WT when valine is present.

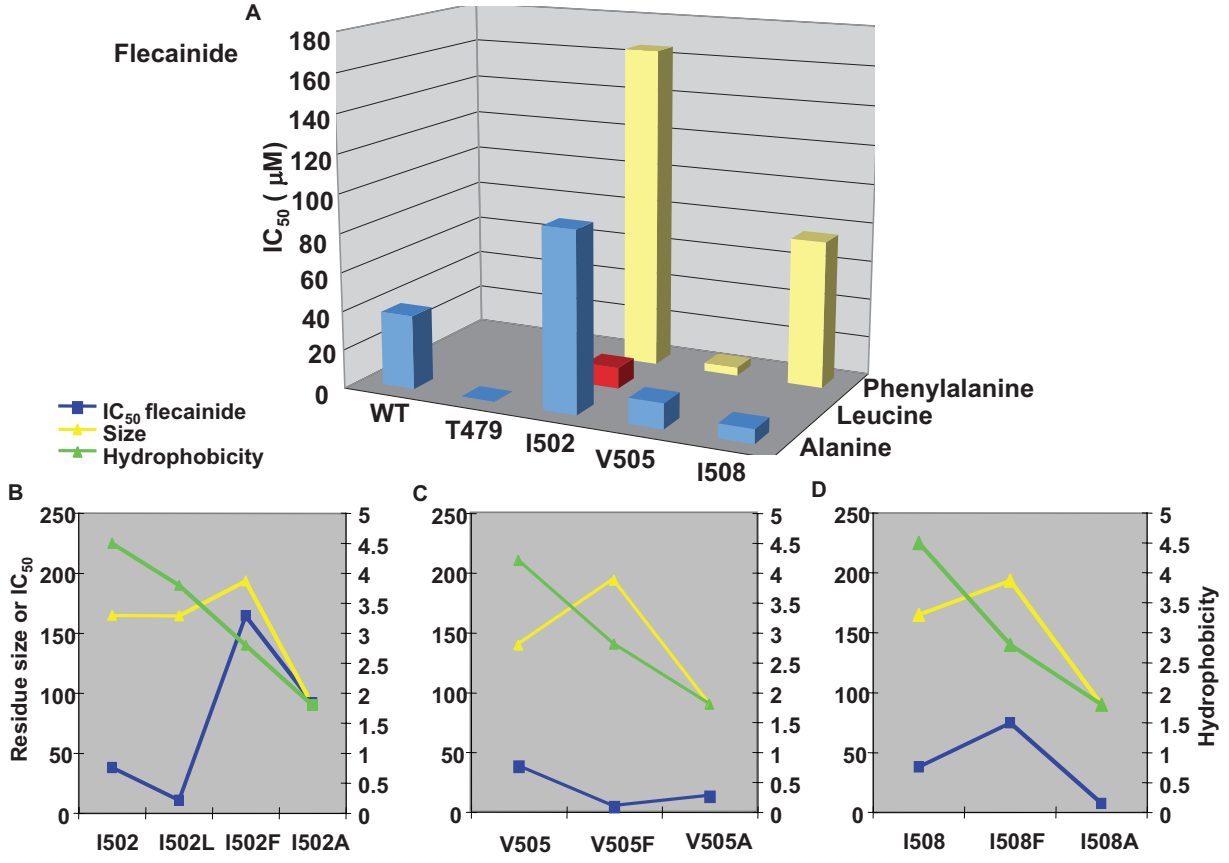

Fig. 6. Various amino acid substitutions to selected residues in S6, and their block by flecainide. A, three-axis graph of the effect of different amino acid substitutions of the WT residues (abscissa) on the resultant mutant Kv1.5 channel IC_{50} (ordinate) for block by flecainide. Note color coding of substituted residues, with WT and alanine mutants in pale blue: red = leucine; yellow = phenylalanine. B–D, correlation graphs comparing flecainide IC_{50} (left ordinate, micromolar) versus hydrophobicity (right ordinate, Kyte-Doolittle units), and size (left ordinate, cubic Ångstroms) for a range of amino acids substituted at Ile502 (B), Val505 (C), and Ile508 (D). Spearman correlation coefficients: for Ile502 for size and hydrophobicity were 0.4, and −0.6, respectively; for Val505, r = −0.5, and 0.5; for Ile508, r = 1.00, and 0.5.

Voltage-Dependent Block of Kv1.5 by Vernakalant and Flecainide. Electrophysiological evidence in support of Ile502 as a critical residue in the interaction of vernakalant with Kv1.5 channels was obtained from studies of the voltage dependence of drug block. As before, comparative experiments were carried out between vernakalant and flecainide (Figs. 7 and 8). In these experiments, cells were exposed to concentrations of vernakalant (Fig. 7) and flecainide (Fig. 8), near their IC_{50} values and depolarized to a range of potentials between −80 and +60 mV as illustrated by the protocol at the top of each figure. Current-voltage relationships were determined for WT and mutant channels (T479A, I502A, V505A, I508A) in the presence of either vernakalant or flecainide (Figs. 7B and 8B). The amount of block was measured at the end of the pulse at the time indicated by the arrow (Figs. 7A and 8A) on each set of data records, and, after normalization to the current density, was plotted as a function of the depolarization potential (Figs. 7C and 8C). Data were then fit to a standard model of drug block to obtain the electrical distance of the blocking site into the electric field from the inside of the channel (Woodhull, 1973). In WT channels, the blocking site was located ~17% of the electrical distance across the membrane (Figs. 7C and 8C), and this was only perturbed in the presence of vernakalant in the I502A mutant, where analysis demonstrated a blocking site ~40% of the electrical distance across the membrane. For flecainide, results were somewhat different. Although I502A did increase the electrical distance to 32%, a significant increase in distance was also observed in V505A. In general, these results strongly support the inner S6 site for the actions of both vernakalant and flecainide but suggest that vernakalant's site of action is very narrowly aligned with Ile502, whereas that of flecainide is more distributed over a couple of turns of the S6 helix from Ile502 to beyond Val505.

These differential effects of alanine substitution on the binding in the S6 region of the channel of vernakalant, flecainide, and some other antiarrhythmic agents [including both Na^+ channel and K^+ channel blockers (Yeola et al., 1996; Decher et al., 2004, 2006; Herrera et al., 2005)] are shown in summary form in Fig. 9, with the structures of the molecules in the bottom panel. It can be seen that AVE0118, which has an apparent maximum molecular length of ~18 Å, exhibits the most significant changes in IC_{50} with mutations between Ile502 and Val512, some four turns of the helix, with minor reductions in potency at Val516. In contrast, the IC_{50} for flecainide (molecular length, 10 Å) is affected by mutations over a narrower range of residues more located in the deep pore. The atrial K^+ channel blocker S0100176 is affected by mutations similarly to AVE0118, but the extent of these effects is more limited, extending from Val505 to Val512, with only minor effects extending to Val516, consistent with the differences in structure between these two

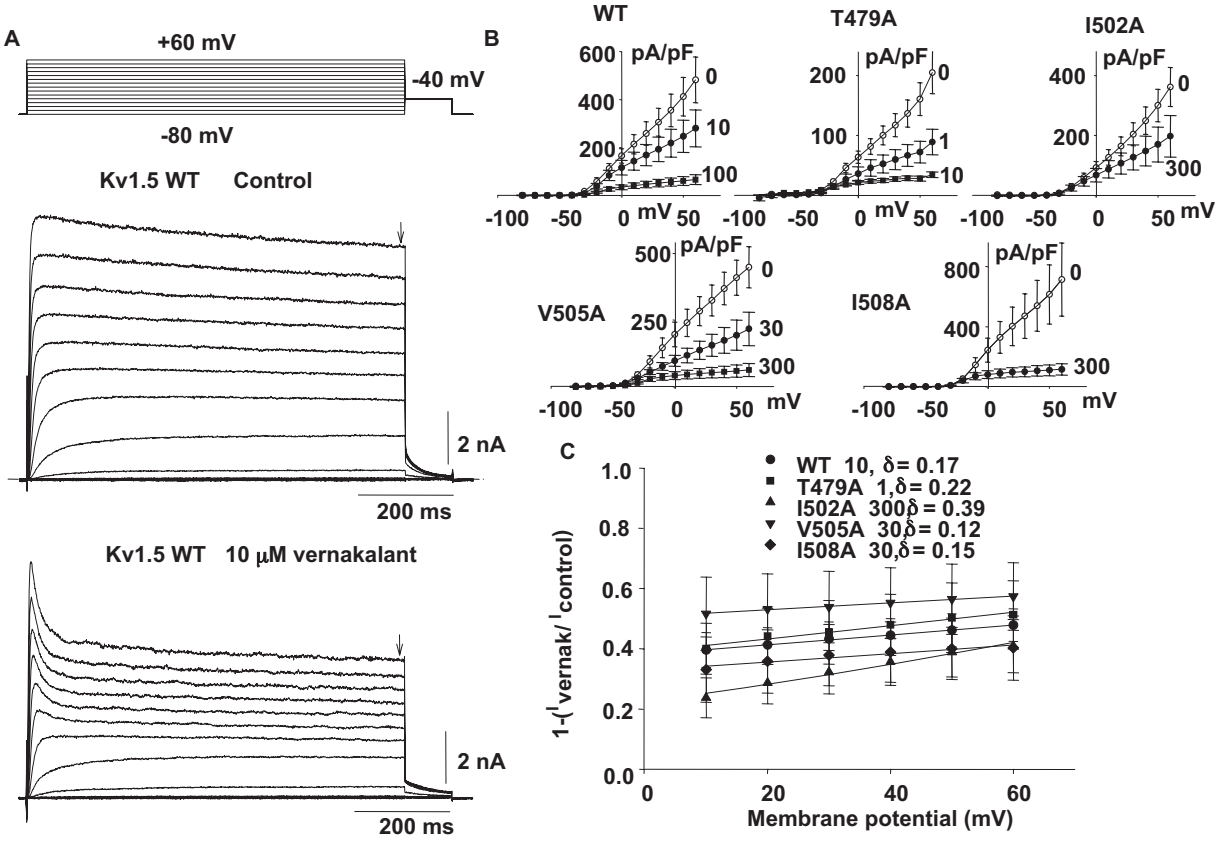

Fig. 7. Voltage-dependent block of selected pore and S6 mutants by vernakalant. A, Kv1.5 current tracings in control (above) and during exposure to 10 μM vernakalant (below) at a range of membrane potentials from −80 to +60 mV, as shown in the protocol at top, data from the same cell. B, current-voltage relationships were obtained from WT and selected mutant Kv1.5 channels at various concentrations. Data points were obtained from experiments carried out as illustrated in A. Currents measured at the end of clamp pulses (at arrows in A) are plotted ± S.E.M. versus voltage clamp step potential for different concentrations of vernakalant (in micromolar). For WT data, n = 12, for T479A, n = 6; for I502A, n = 6; for V505A, n = 8; for I508A, n = 8. C, normalized voltage-dependent block is plotted versus clamp potential and fitted with a Woodhull equation to calculate the fractional electrical distance of drug binding (δ; see inset legend for values and *Materials and Methods* for explanation).

drugs (Decher et al., 2006). There are also differential effects of mutations between drugs thought to act primarily on Na^+ channels and those with more dominant K^+ channel actions (Fig. 9). Flecainide and quinidine show increases in potency with mutations in the lower part of S6 between position 503 and 516, whereas those drugs that are more potent on K^+ channels, including vernakalant, AVE0118, and S0100176, all show decreases in potency with mutations throughout the same region (Fig. 9). However, unlike AVE0118, S0100176, and quinidine, T479A increased vernakalant and flecainide sensitivity, suggesting a common interaction at this site.

Structural Considerations from Homology Modeling. Mutations at Cys500 and Ala501 both resulted in significant, though opposite, changes in IC_{50} for vernakalant (Table 1); in contrast, no differences were observed for AVE0118 and S0100176 (Decher et al., 2004, 2006) (Fig. 9). A homology model of Kv1.5 based on Kv1.2 (Long et al., 2005) was constructed (Fig. 10), and this puts these two residues at the base of the pore helix with a predicted H-bond between Cys500 and Thr477 in the adjacent helix (Fig. 10C). Mutation of the analogous residue in Kv2.1 (C393A) affected the stability of the open state and ion permeation without affecting external or internal tetraethylammonium block (Liu and Joho, 1998). The A501V mutation had the most dramatic effects on inactivation and was one of the more sensitive mutants to vernakalant (Fig. 2, and Table 1), and it is possible that disruption of the putative H-bond, with a subsequent change of inactivation gating is responsible, at least in part, for the potency increase and the differential effect of vernakalant on this residue compared with Ala501.

In the homology model of Kv1.5, the side chains of Ile502 appear to point away from the internal cavity of the vestibule and toward two highly conserved leucines (Leu437 and Leu441; Fig. 10, A and B) in an adjacent subunit (Fig. 10B), which makes it interesting that mutations at this site have such large effects on drug affinity. How might mutation at this residue affect drug affinity? Given that potential interactions between Ile502 and the leucines in the adjacent subunit would involve hydrophobic interactions, changes in hydrophobicity at Ile502 might interfere with subunit packing and thus alter the binding site via an allosteric mechanism. Depending on the number of other interactions between the drug and the channel and the strength of these interactions, the changes around Ile502 may have greater or lesser affects. At this site, changes are more dramatic for vernakalant than for AVE0118, which interacts over a greater number of residues within the channel (Fig. 9), consistent with its more extended configuration (~18 Å).

Molecular Docking of Vernakalant in Kv1.2. In an attempt to predict the vernakalant binding site in Kv1.5, the crystallized pore region of Kv1.2 (Long et al., 2005) was

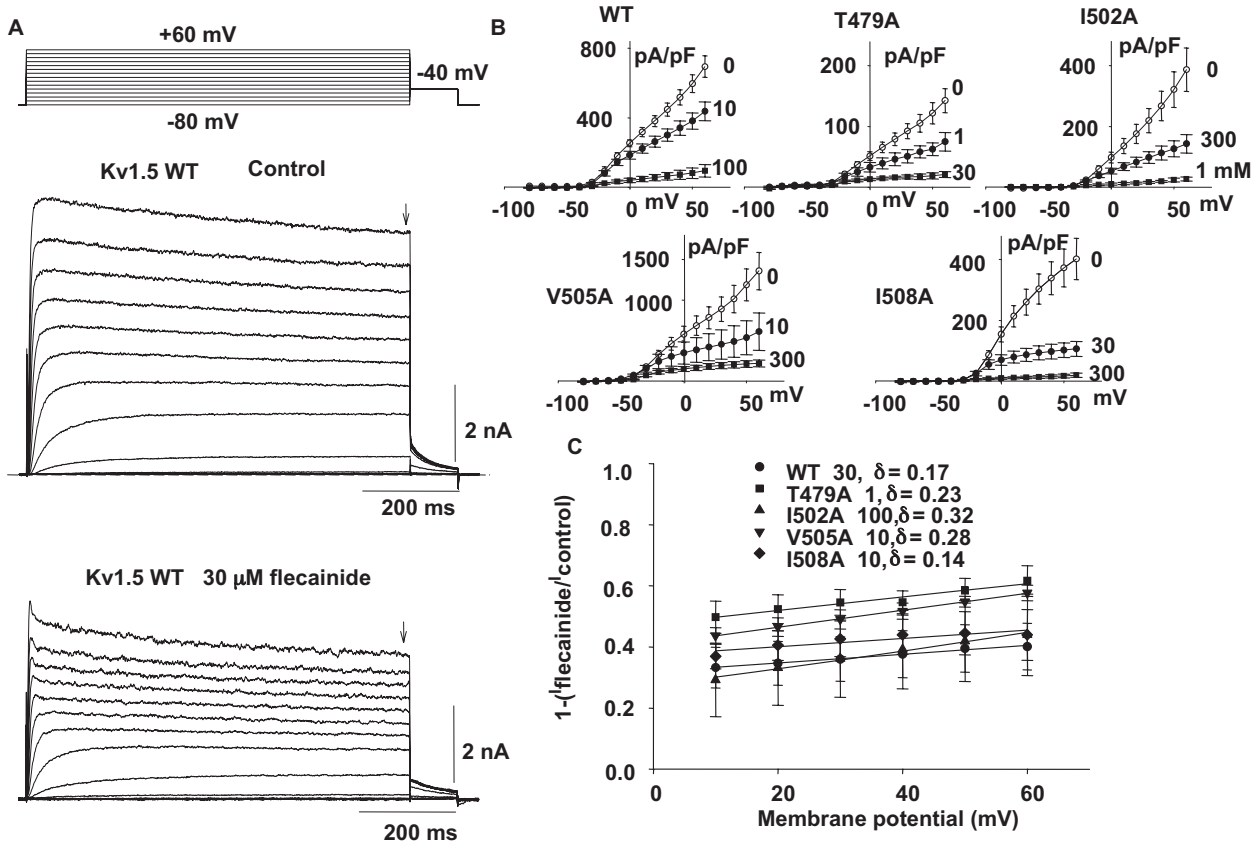

Fig. 8. Voltage-dependent block of selected pore and S6 mutants by flecainide. A, Kv1.5 current tracings in control (above) and during exposure to 30 μM flecainide (below) at a range of membrane potentials from −80 to +60 mV, as shown in the protocol at top, data from the same cell. B, current-voltage relationships obtained from WT and selected mutant Kv1.5 channels as labeled on each graph. Data points were obtained from experiments carried out as illustrated in A. Currents measured at the end of clamp pulses (at arrows in A) are plotted ± S.E.M. versus voltage clamp step potential for different concentrations of flecainide (in micromolar). For WT data, $n = 12$, for T479A, $n = 6$; for I502A, $n = 6$; for V505A, $n = 8$; for I508A, $n = 8$. C, normalized voltage-dependent block is plotted versus clamp potential and fitted with a Woodhull equation to calculate the fractional electrical distance of drug binding (δ; see inset legend for values and *Materials and Methods* for explanation).

used with an energy-minimized conformation of vernakalant (Fig. 11). Using AutoDock tools, a docking grid was built that encompassed the entire pore region of the channel, for the macromolecule, and a ligand-docking grid that included the complete structure of vernakalant. Ten energy-minimized docking conformations were obtained from the AutoDock program; the most stable conformation is illustrated in Fig. 11. This view of the channel pore shows only those residues predicted to interact with vernakalant, except for Ile502, which does not interact but is shown in its position facing away from the vestibule. The view is from the cytoplasmic surface and reveals residues in S6, Val505, and Ile508 that are predicted to interact with vernakalant, as well as residues at the base of the

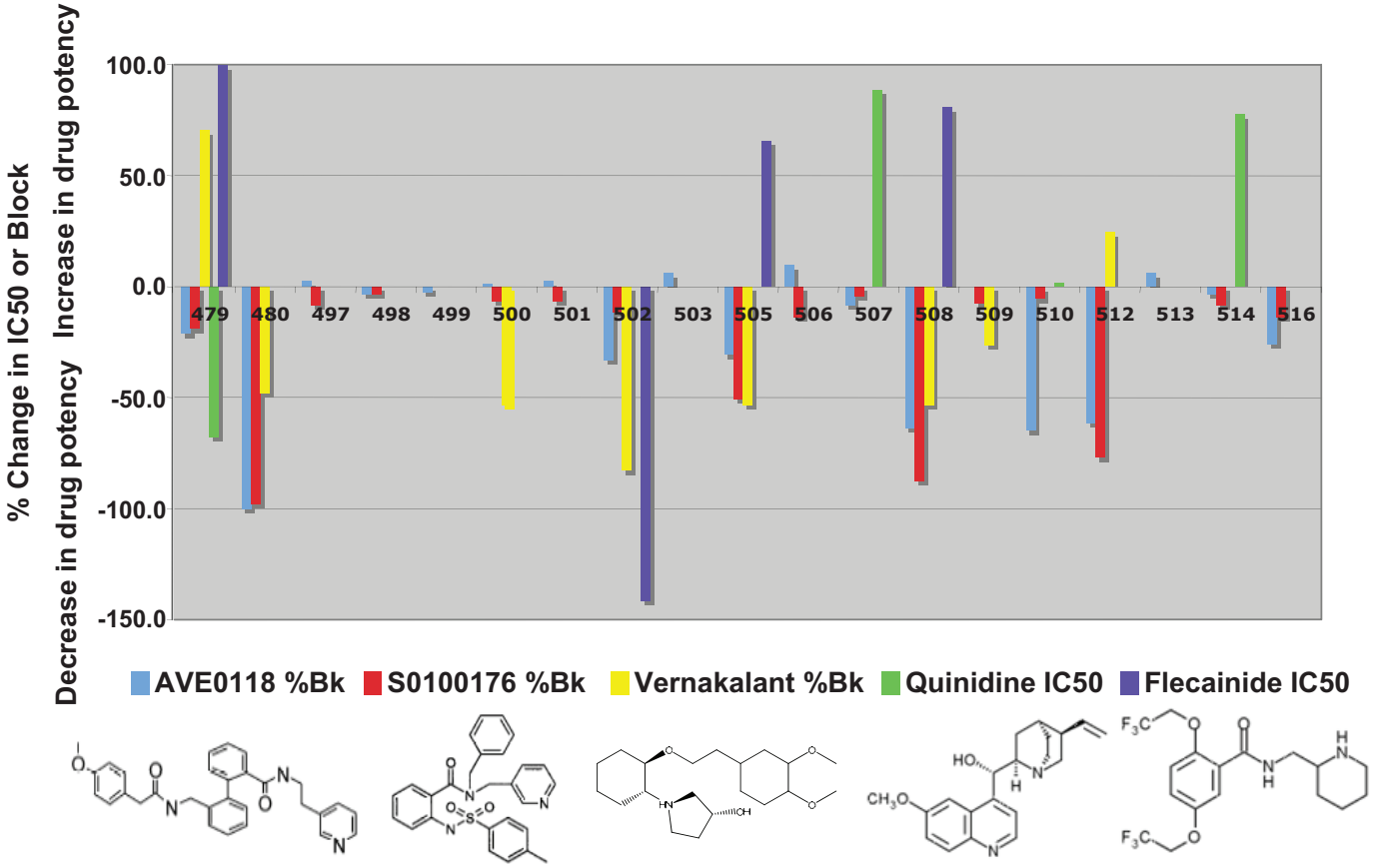

Fig. 9. Comparison of effects of alanine substitution on block of Kv1.5 by vernakalant, flecainide, and other antiarrhythmic agents. Percentage changes in IC_{50} or fractional block were calculated from derived data (vernakalant and flecainide) or from values obtained from available published work involving alanine mutations (see *Results* for details). Molecular structures of the five compounds are shown in the bottom panel. Note that at residue 501, the mutation was an alanine to a valine

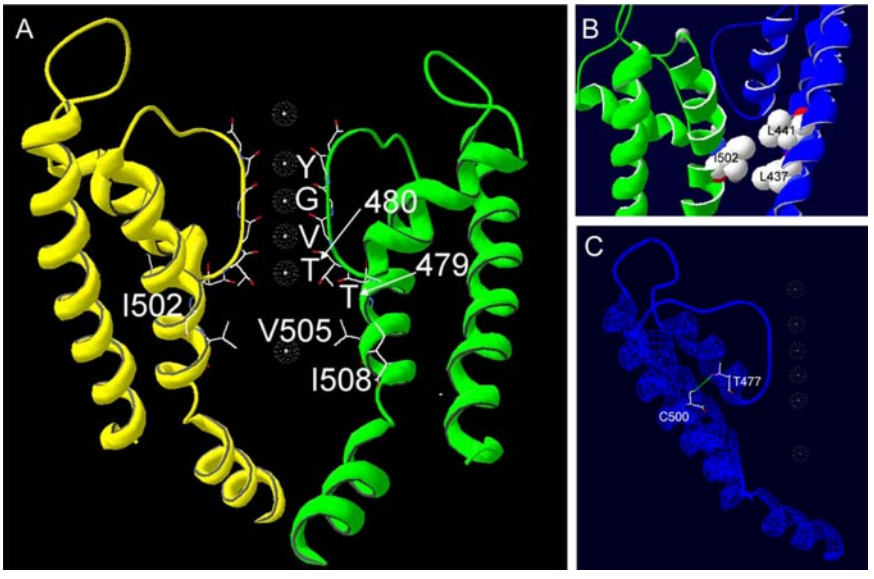

Fig. 10. Kv1.5 pore homology model illustrating residues that when mutated altered sensitivity to block by vernakalant. A, Kv1.5 homology model was generated for the S5-p-loop-S6 region based on the crystal structure for Kv1.2. A, the model shows side chains for residues Thr479, Thr480, Ile502, Val505, and Ile508. B, the side chain of Ile502 appears to point toward Leu437 and Leu441 (shown in space fill representation) in the adjacent subunit. C, homology model predicts an H-bond between Cys500 in S6 and Thr477 in the pore helix.

pore helix, Thr480 and Met478, that also interact with the compound. Thr480 in all four subunits, in this view, marks the narrowest point of the deep pore at the selectivity filter. In this docking conformation, vernakalant appears to be folded in upon itself, with its ether linkage facing the Thr480 of three subunits (green, magenta, and white) at the base of the selectivity filter. The cyclohexane ring on one side of the ether linkage of vernakalant coordinates with Val505 of two subunits (green and magenta), and the attached dimethoxy groups lie with Val505 and Ile508 in the same subunit. The phenyl ring of vernakalant interacts closely with Val505 and Ile508, predominantly in the white subunit. The pyrrolidine ring (cyclic amine) and its attached hydroxyl group interact with Val505 and Ile508. In the other energy-minimized docking conformations, many of the same amino acids as those shown in Fig. 11 were modeled to interact with vernakalant.

Overall, this docking conformation of vernakalant in the pore of Kv1.5 gives excellent agreement with the experimental predictions from mutational studies described above, highlighting as it does the threonine residue at the base of the pore helix (Thr480) and Val505 and Ile508 in the S6.

Vernakalant Block of Other Voltage-Gated Ion Channels. An alignment of a range of voltage-gated potassium channels for the S5, selectivity filter, and S6 regions is shown in Fig. 12. It can be seen that at the equivalent position of Ile502, in most of the Kv3 and Kv4 channels, as well as hERG channels, there is a leucine. In our present studies, substitution of isoleucine with leucine decreased the sensitivity of Kv1.5 to 24.8 μM, and this is close to the reported sensitivity of Kv4 and hERG channels for vernakalant (Fedida et al., 2005). Another possible explanation for the difference in the latter case may be the presence of the tyrosine at the equivalent position to Ile508 in hERG. I508Y in our experiments increased the IC_{50} for vernakalant on Kv1.5 to 24.7 μM (Table 1), again similar to the reported value for hERG. This tyrosine, along with a phenylalanine at the equivalent position of Val512 in Kv1.5 (Fig. 12), has been implicated in the binding of several classes of drug to hERG, leading to acquired long QT syndrome, as reviewed by Sanguinetti and Mitcheson (2005). Thus, the reduced potency for vernakalant on K^+ channels other than Kv1.5 may reflect, at least in part, the three-dimensional structural differences inferred from the present study.

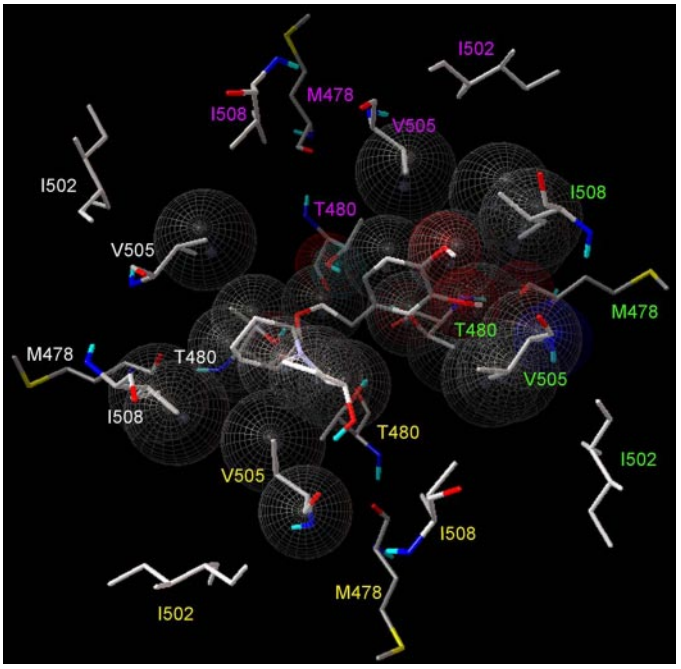

Fig. 11. Lowest energy docking conformation of vernakalant displayed with interacting residues of Kv1.5. This conformation shows the drug-interacting residues on the four channel subunits as predicted by the model. The view is from the cytoplasmic side of the channel, looking up into the open pore and selectivity filter. Residues and conformations were predicted by AutoDock4 using the crystal structure of rKv1.2 (Protein Data file 2A79; Long et al., 2005). The channel structure was kept rigid and vernakalant allowed to be flexible. Different colors were used to label amino acids from each subunit of the channel tetramer. Ile502 was added to the figure although it was not predicted to be an interacting residue. The large spheres are space-filled representations of specific atoms. Carbons are shown as gray, oxygen as red, hydrogen as blue/green, and nitrogen as dark blue.

Discussion

In this study we have examined the binding of the novel atrial antiarrhythmic agent, vernakalant, to the Kv1.5 channel which underlies the rapidly activating atrial K^+ current, I_{Kur}. Previous work had suggested that channel activation was required for drug action (Fedida et al., 2005), and in support of this, as also described for AVE0118 (Decher et al., 2006), vernakalant was shown to slow channel closing by hindering movement of the deactivation gate, like a 'foot-in-the-door' (Fig. 1). This initial observation allowed us to narrow the scope of our mutational analysis of the drug binding site to the inner vestibule and deep pore of the channel.

Findings from the Alanine Scan. An alanine scan of residues in the deep pore/pore helix (Thr479–Val481) and lower S6 (Cys500–Val512) was carried out, although the mutations here were limited somewhat based on the crystal structure of Kv1.2 (Long et al., 2005) to those that were predicted to face the inner cavity, except for Ile502. Where the literature indicated that an alanine was incompatible with expression, we made other changes as summarized in Table 1. The results of this mutational scan of the Kv1.5 deep pore and S6 domains show a great deal of overlap with key residues shown to be involved in block by other compounds (Yeola et al., 1996; Caballero et al., 2002; Decher et al., 2004, 2006; Herrera et al., 2005). This is not surprising given the limited number of amino acid side chains that will project into the inner cavity and be available for interaction with a candidate blocker. Mutations that resulted in a significant change in the vernakalant IC_{50} involved residues Thr479, Thr480, Cys500, Ala501, Ile502, Val505, Ile508, and Pro532. Despite the overlap in binding sites, there are apparent differences in both the importance of various residues to block by the various compounds [compare changes in IC_{50} for vernakalant and flecainide with mutation at Ile502, Val505, and Ile508 (Figs. 5 and 6)] and in the distance along S6 involved (Fig. 9). Block by both AVE0118 and S0100176 is affected by mutations at Leu510, Val512, and Val516 (Decher et al., 2004, 2006). Although Leu510 and Val516 were not screened in the present study, the lack of significant difference in block by vernakalant beyond Ile508 (Fig. 2) [with the particular exception of P532L (see below)] suggests a minor role of those residues in vernakalant's interaction with the channel. We

have shown that residue Ile502 appears to be a special case in that although mutations to this residue had large effects on the potency of vernakalant action, it appears to face away from the cavity and, indeed, homology docking (Fig. 11) indicated no direct interaction of the residue with vernakalant.

Other Amino Acid Substitutions Give Further Information on Vernakalant Binding in the S6. Several further mutations were made at the key residues identified by the alanine scan (Fig. 5 and Table 1). The more conservative threonine-to-serine mutations at 479 and 480 result in a reduction in side chain volume similar to that caused by alanine but maintain the polar hydroxyl group. Both of these mutations decreased the potency of the drug (Fig. 5A) and resulted in WT-like inactivation rates (data not shown). The minimized energy docking predicts significant interactions between Thr480 with the 6-carbon rings of vernakalant (Fig. 11), but Thr479 is also likely to contribute to K^+ coordination (Zhou and MacKinnon, 2004), so mutations here may be having multiple effects on permeation with downstream effects on inactivation. In oocytes, a V481L mutation also made Kv1.5 more sensitive to flecainide without affecting inactivation (Herrera et al., 2005), despite evidence suggesting that this residue is important for K^+ coordination (Long et al., 2005). As shown in Table 1, we saw a significant increase in potency on mutation of Thr479 to an alanine but not for the V481L mutation. T479A has the additional affect of enhancing C-type inactivation (Fig. 2B), which complicates interpretation of the changes in IC_{50}. It is interesting to note that this mutation does not have the same effect on drug block by all compounds studied, with some becoming more potent (vernakalant and flecainide; Tables 1 and 2) and others less so [AVE0118, S0100176, and quinidine (Yeola et al., 1996; Decher et al., 2004, 2006); Fig. 9].

Ile502: Potential Hydrophobic Interactions in S5? At Ile502, insertion of a phenylalanine residue (Phe) capable of π-stacking appeared unable to facilitate vernakalant block. Rather, the IC_{50} at Ile502 was inversely related to hydrophobicity (Fig. 5A), highlighting the potential hydrophobic interactions with Ile502 in determining inner vestibule architecture. Because Ile502 is predicted to point away from the inner cavity of the channel, we have hypothesized in our homology modeling that interactions of Ile502 with leucines 437 and 441 in the adjacent S5 subunit play a significant role in determining such interactions (Figs. 10 and 11). It is noteworthy that the IC_{50} of flecainide was increased more by this mutation than by the alanine (Fig. 6), perhaps indicating some steric effects of this mutation. The importance of Ile502 in flecainide block has been studied previously (Herrera et al., 2005). In that study, the I502L mutation was adequate for rendering Kv1.5 as sensitive to flecainide as Kv3.1 and Kv4.2. Those studies were carried out using *Xenopus laevis* oocytes and thus the exact IC_{50} values are different, but the trend was the same as observed in the HEK cells used in our study.

Further evidence that the residue Ile502 is of importance in regulating the potency of vernakalant action on Kv1.5 was obtained from electrophysiological studies of the voltage-dependence of block (Figs. 7 and 8). Here it was found that the mutation I502A shifted the calculated binding site of vernakalant within the electric field from 0.17 to 0.39 of the way across the electric field from the inside of the pore. This action of I502A was unique for the sites tested in this manner for vernakalant and suggests that the mutation was able to specifically disrupt high affinity access of the drug to the permeation pathway, as the IC_{50} for block was reduced 25-fold in this mutant (Fig. 3). The increased electrical distance that results from the mutation may reflect a deeper penetration of the drug into the inner vestibule after loss of its coordinated site and an upper limit of intracellular access of the drug due to the proximity of the narrowing of the selectivity filter. If vernakalant is now moving deeper into the pore, the increase in IC_{50} may also reflect competition with K^+ for interaction with residues at the base of the filter. In comparison, the similar mutation for flecainide did not change the electrical distance as much (0.32 versus 0.17), and the potency of block was only altered 2.4-fold (Fig. 4). In flecainide, the V505A mutation was able to induce a similar, if opposite change in potency to I502A, which suggests that flecainide binding to the channel is coordinated along a broader region of S6 than vernakalant and in a less critical manner by the isoleucine at position 502 and the valine at position 505

Additional mutations at Val505 and Ile508 resulted in further changes in IC_{50} (Figs. 5 and 6) and mostly tracked with changes in size, although flecainide in particular may be capable of cation-π-stacking interactions with an aromatic amino acid placed at Val505 but not at Ile508. A hydrophobic aromatic amino acid more distant from the pore appears more favorable for block by vernakalant (compare I508F and I508Y in Fig. 5). These mutations are of particular interest, because the equivalent residues in the proteins underlying the ventricular delayed rectifier currents I_{Ks} (KvLQT1) and

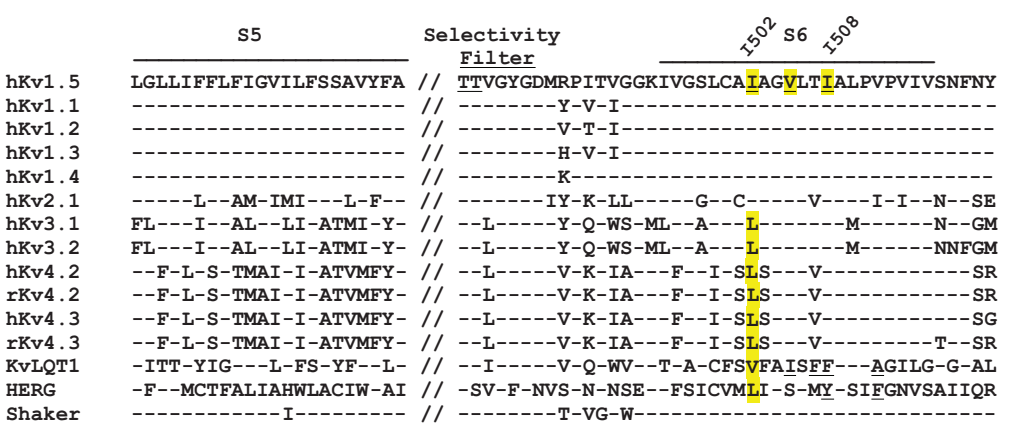

Fig. 12. Alignment of S5, pore, and S6 regions from a number of potassium channels. Alignment of potential pore interaction regions from a variety of K channels. //, omitted sequence in the pore turret; -, identical residues in different channels. The span of the S5, selectivity filter, and S6 regions are identified by the solid black bars above the sequence. Residues Ile502, Val505, and Ile508 are identified by highlighting in the top row for Kv1.5 and the Ile502 equivalent residue in the other channels. Underscored residues in KvLQT1 and hERG channel genes are discussed under *Results*.

I_{Kr} (hERG) are phenylalanine and tyrosine, respectively (Fig. 12). Although the I508Y mutant has a similar IC_{50} to hERG (Fedida et al., 2005), data for I_{Ks} show that this channel does not seem to be sensitive to vernakalant (M. Pourrier, unpublished data) indicating that the extensive sequence differences between this channel and Kv1.5 (Fig. 12) make any predictions difficult.

Several other mechanisms exist by which a given mutation could affect drug block, including: 1) loss of a side-chain quality needed for direct interaction with the drug (hydrophobic, electrostatic, π-stacking); 2) local or global changes in the binding site without the residue making direct contact with the drug itself; 3) a steric effect, with the mutation blocking access to the binding site; and 4) a change in the gating state of the channel. A naturally occurring polymorphism in Kv1.5, P532L, appears to have steric effects on quinidine (Drolet et al., 2005) and propafenone access (Simard et al., 2005). Quinidine traversed the same distance across the electric field to block Kv1.5 channels with the P532L mutation, suggesting that the binding site was not affected. However, block was reduced and evidence suggested that in the absence of the proline, a helix might form and impede access to the inner vestibule (Drolet et al., 2005). It appears that this mutation may have a similar effect on access for vernakalant (Fig. 2L).

Acknowledgments

We thank Fifi Chiu and Kyung Hee Park for help with cell culture and cloning of mutant channels. We thank Dr. David Steele for molecular support, primer design, and cloning and Dr T. Claydon for homology modeling. We thank Dr. Grace Jung for help with the energy-minimized form of vernakalant.

References

Caballero R, Moreno I, Gonzalez T, Valenzuela C, Tamargo J, and Delpon E (2002) Putative binding sites for benzocaine on a human cardiac cloned channel (Kv1.5). *Cardiovasc Res* **56:**104–117.

Choi KL, Mossman C, Aubé J and Yellen G (1993) The internal quaternary ammonium receptor site of *Shaker* potassium channels. *Neuron* **10:**533–541.

Decher N, Kumar P, Gonzalez T, Pirard B, and Sanguinetti MC (2006) Binding site of a novel Kv1.5 blocker: a "foot in the door" against atrial fibrillation. *Mol Pharmacol* **70:**1204–1211.

Decher N, Kumar P, Gonzalez T, Renigunta V, and Sanguinetti MC (2005) Structural basis for competition between drug binding and Kvβ 1.3 accessory subunit-induced N-type inactivation of Kv1.5 channels. *Mol Pharmacol* **68:**995–1005.

Decher N, Pirard B, Bundis F, Peukert S, Baringhaus KH, Busch AE, Steinmeyer K, and Sanguinetti MC (2004) Molecular basis for Kv1.5 channel block: conservation of drug binding sites among voltage-gated K^+ channels. *J Biol Chem* **279:**394–400.

Drolet B, Simard C, Mizoue L, and Roden DM (2005) Human cardiac potassium channel DNA polymorphism modulates access to drug-binding site and causes drug resistance. *J Clin Invest* **115:**2209–2213.

Fedida D (1997) Gating charge and ionic currents associated with quinidine block of human Kv1.5 delayed rectifier channels. *J Physiol* **499:**661–675.

Fedida D (2007) Vernakalant (RSD1235): a novel, atrial-selective antifibrillatory agent. *Expert Opin Investig Drugs* **16:**519–532.

Fedida D, Orth PMR, Chen JYC, Lin S, Plouvier B, Jung G, Ezrin A, and Beatch GN (2005) The mechanism of atrial antiarrhythmic action of RSD1235. *J Cardiovasc Electrophysiol* **16:**1227–1238.

Fedida D, Wible B, Wang Z, Fermini B, Faust F, Nattel S, and Brown AM (1993) Identity of a novel delayed rectifier current from human heart with a cloned K^+ channel current. *Circ Res* **73:**210–216.

Feng JL, Wible B, Li GR, Wang ZG, and Nattel S (1997) Antisense oligodeoxynucleotides directed against Kv1.5 mRNA specifically inhibit ultrarapid delayed rectifier K^+ current in cultured adult human atrial myocytes. *Circ Res* **80:**572–579.

Franqueza L, Longobardo M, Vicente J, Delpón E, Tamkun MM, Tamargo J, Snyders DJ, and Valenzuela C (1997) Molecular determinants of stereoselective bupivacaine block of hKv1.5 channels. *Circ Res* **81:**1053–1064.

Fuster V, Ryden LE, Cannom DS, Crijns HJ, Curtis AB, Ellenbogen KA, Halperin JL, Le Heuzey JY, Kay GN, Lowe JE, et al. (2006) ACC/AHA/ESC 2006 Guidelines for the Management of Patients with Atrial Fibrillation: a report of the American College of Cardiology/American Heart Association Task Force on Practice Guidelines and the European Society of Cardiology Committee for Practice Guidelines (Writing Committee to Revise the 2001 Guidelines for the Management of Patients With Atrial Fibrillation): developed in collaboration with the European Heart Rhythm Association and the Heart Rhythm Society [published erratum appears in *Circulation* **116:**e138, 2007]. *Circulation* **114:**e257–e354.

Go AS, Hylek EM, Phillips KA, Chang Y, Henault LE, Selby JV, and Singer DE (2001) Prevalence of diagnosed atrial fibrillation in adults: national implications for rhythm management and stroke prevention: the AnTicoagulation and Risk Factors in Atrial Fibrillation (ATRIA) Study. *JAMA* **285:**2370–2375.

Grissmer S, Nguyen AN, Aiyar J, Hanson DC, Mather RJ, Gutman GA, Karmilowicz MJ, Auperin DD, and Chandy KG (1994) Pharmacological characterization of five cloned voltage- gated K^+ channels, types Kv1.1, 1.2, 1.3, 1.5, and 3.1, stably expressed in mammalian cell lines. *Mol Pharmacol* **45:**1227–1234.

Herrera D, Mamarbachi A, Simoes M, Parent L, Sauve R, Wang Z, and Nattel S (2005) A single residue in the S6 transmembrane domain governs the differential flecainide sensitivity of voltage-gated potassium channels. *Mol Pharmacol* **68:**305–316.

Holmgren M, Shin KS, and Yellen G (1998) The activation gate of a voltage-gated K^+ channel can be trapped in the open state by an intersubunit metal bridge. *Neuron* **21:**617–621.

Kannel WB, Wolf PA, Benjamin EJ, and Levy D (1998) Prevalence, incidence, prognosis and predisposing conditions for atrial fibrillation: population based estimates. *Am J Cardiol* **82:**2N–9N.

Kirsch GE and Drewe JA (1993) Gating-dependent mechanism of 4-aminopyridine block in two related potassium channels. *J Gen Physiol* **102:**797–816.

Leung JM, Bellows WH, and Schiller NB (2004) Impairment of left atrial function predicts post-operative atrial fibrillation after coronary artery bypass graft surgery. *Eur Heart J* **25:**1836–1844.

Liu Y and Joho RH (1998) A side chain in S6 influences both open-state stability and ion permeation in a voltage-gated K^+ channel. *Pflugers Arch* **435:**654–661.

Long SB, Campbell EB, and MacKinnon R (2005) Crystal structure of a mammalian voltage-dependent *Shaker* family K^+ channel. *Science* **309:**897–903.

Lopez GA, Jan YN, and Jan LY (1994) Evidence that the S6 segment of the *Shaker* voltage-gated K^+ channel comprises part of the pore. *Nature* **367:**179–182.

Morris GM, Goodsell DS, Halliday RS, Huey R, Hart WE, Belew RK, and Olson AJ (1998) Automated docking using a Lamarckian genetic algorithm and an empirical binding free energy function. *J Comput Chem* **19:**1639–1662.

Persson F, Carlsson L, Duker G, and Phd IJ (2005) Blocking characteristics of hKv1.5 and hKv4.3/hKChIP2.2 after administration of the novel antiarrhythmic compound AZD7009. *J Cardiovasc Pharmacol* **46:**7–17.

Pratt C, Roy D, Juul-Moller S, et al., on behalf of the ACT III Investigators (2006) Efficacy and tolerance of RSD1235 in the treatment of atrial fibrillation or atrial flutter: results of a phase III, randomized, placebo-controlled, multicenter trial (Abstract). *J Am Coll Cardiol* **47** (Suppl A)**:**10A.

Rockson SG and Albers GW (2004) Comparing the guidelines: anticoagulation therapy to optimize stroke prevention in patients with atrial fibrillation. *J Am Coll Cardiol* **43:**929–935.

Roy D, Pratt C, Wyse DG, Toft E, Torp-Pedersen C, and Juul-Moller S (2005) Efficacy and Safety of RSD1235 in the treatment of recent onset atrial fibrillation in ACT I (Atrial Arrhythmia Conversion Trial I), a phase III, randomized, placebo-controlled, multi-center trial. European Society of Cardiology Annual Congress; 3–7 Sep 2005; Stockholm, Sweden. Abstract P3045. Available at http://spo.escardio.org/AbstractDetails.aspx?id=24704

Roy D, Rowe BH, Stiell IG, Coutu B, Ip JH, Phaneuf D, Lee J, Vidaillet H, Dickinson G, Grant S, et al. (2004) A randomized, controlled trial of RSD1235, a novel anti-arrhythmic agent, in the treatment of recent onset atrial fibrillation. *J Am Coll Cardiol* **44:**2355–2361.

Sanguinetti MC and Mitcheson JS (2005) Predicting drug-hERG channel interactions that cause acquired long QT syndrome. *Trends Pharmacol Sci* **26:**119–124.

Simard C, Drolet B, Yang P, Kim RB, and Roden DM (2005) Polymorphism screening in the cardiac K^+ channel gene KCNA5. *Clin Pharmacol Ther* **77:**138–144.

Snyders DJ, Knoth KM, Roberds SL, and Tamkun MM (1992) Time-, voltage-, and state-dependent block by quinidine of a cloned human cardiac potassium channel. *Mol Pharmacol* **41:**322–330.

Stiell IG, Roy D, Rowe BH, Pratt C, Dickinson G, and Kitt T (2006) Efficacy and safety of RSD1235 in the treatment of acute atrial fibrillation (Abstract). *Acad Emerg Med* **13 (Suppl 1):**S162-a.

Woodhull AM (1973) Ionic blockage of sodium channels in nerve. *J Gen Physiol* **61:**687–708.

Yeola SW, Rich TC, Uebele VN, Tamkun MM, and Snyders DJ (1996) Molecular analysis of a binding site for quinidine in a human cardiac delayed rectifier K^+ channel—role of S6 in antiarrhythmic drug binding. *Circ Res* **78:**1105–1114.

Zhou Y and MacKinnon R (2004) Ion binding affinity in the cavity of the KcsA potassium channel. *Biochemistry* **43:**4978–4982.

Address correspondence to: Dr. David Fedida, Department of Anesthesiology, Pharmacology, and Therapeutics, University of British Columbia, 2176 Health Sciences Mall, Vancouver BC, Canada V6T 1Z3. E-mail: fedida@interchange.ubc.ca